A mixed methods approach to reconstructing hydrographs of an extreme flood in an ungauged catchment in Ostional, Nicaragua

Shannon L. Jones[1,2*] and Heyddy Calderón[3]

[1] Geography and the Environment, University of Denver, CO, USA
[2] Environmental Sciences Division, Oak Ridge National Laboratory, TN, USA
[3] Ministerio del Ambiente y los Recursos Naturales, Managua, NI

[*]Corresponding authors: Shannon L. Jones, jonessl@ornl.gov; Heyddy Calderón, heyddy.calderon@gmail.com

Submitted to Water Resource Research, Aug 2023

Highlights:

- Water resource management, particularly for critical infrastructure, can be improved using a mixed methods approach to provide knowledge of the upper limit of flooding.
- Paleoflood data can be verified and constrained using household survey data and channel cross-sections to improve peak streamflow estimates in in ungauged catchments in data-limited regions.
- Detailed survey data that incorporates local knowledge to bridge gaps in traditional hydrometeorological and modeling methods helps distinguish timing, magnitude and duration of extreme floods in multiple river reaches.

Abstract: Annually, flooding causes major economic losses and affects millions of people worldwide. However, flood-prone regions with insufficient hydrological information typically suffer the greatest flood impacts. These regions are often hard-to-access, lack human and financial resources, and have limited or erroneous flood information. Alternatively, non-instrumental data sources can provide knowledge of the local hydrology. Paleohydrology landscape evidence of past major floods can estimate the most extreme flood discharge within a catchment. Human observations can constrain this value and provide reliable estimates on flood duration, flow paths, and geomorphic impacts. This study uses mixed paleohydrology and human observational methods in a representative ungauged catchment in Ostional, Nicaragua after an extreme flood in October 2017. To estimate daily-to-hourly flood information from mean survey responses and reconstruct storm hydrographs of the upper, middle, and lower reaches, 32 household surveys were conducted. Household survey results supported paleoflood data and provided important hydrograph components, such as lag time and shape, often missing in ungauged catchments. Incorporating human observations into hydrological analyses enhances scientific understanding by providing perspectives of flooding rarely incorporated into research and by providing a voice for inhabitants affected by flooding. Although it is not possible to distinguish between spatial and human ambiguity, this information is highly valuable to improve understanding of extreme and flash flood events not typically captured in traditional hydrometeorological and streamflow monitoring methods. Our mixed-methods approach has significant potential for improving the reliability of current flood assessments and predictions for better flood management in any data-limited region around the world.

Plain Language Abstract: Flooding is a major problem that affects many people and causes economic losses worldwide. Unfortunately, areas with little or no flood information suffer the most from these disasters. These regions are often difficult to reach, lack financial resources, and have limited personnel, which leads to a lack of monitoring sites and data. This results in inaccurate flood information. However, we can use alternative sources of data to fill these gaps. By studying evidence of past floods, known as paleohydrology proxy records, we can estimate the most extreme flood discharge that has occurred in a

watershed. Combining this information with observations from local residents can provide reliable estimates of storm and flood characteristics. In our study conducted in Ostional, Nicaragua, we used a mixed methods approach after a severe flood in 2017. We conducted household surveys and collected data from paleoflood records to reconstruct the storm's impact. The survey results supported the paleoflood data and provided valuable information about the flood, such as timing and shape, which is often missing in areas without monitoring. Including human observations in hydrological analyses improves our understanding of flooding and gives a voice to those affected by floods. Although we can't separate spatial and human factors, this information is valuable for improving flood assessments and predictions in regions with limited data. Our approach has the potential to enhance flood management worldwide.

Keywords: extreme flood, paleoflood hydrology, human observations, hydrograph, ungauged catchment, data-limited regions

1. Introduction

Consistently identified as one of the greatest natural hazards, flooding affects millions of people worldwide and estimated annual economic damages of billions of US dollars (NCEI, 2021). These damages are expected to increase with increased frequency and severity of floods by the mid-21st century (IPCC, 2019). To reduce current and minimize future flood risks, an effective understanding of drivers and impacts of floods are needed to inform decision making. Yet, flood-prone regions with limited hydrometeorological data often suffer the most severe impacts from floods (Walker et al., 2016).

Hydrologic processes in these data-limited regions can be difficult to characterize due to several factors, including insufficient human and financial resources, many ungauged catchments, difficult-to-access terrain, and sparsely placed, shorter-term monitoring sites (Kundzewicz, 2007; Wohl et al., 2012; Zheng et al., 2018; Gorgoglione et al., 2020; Nigussie et al., 2020). These constraints result in spatial and temporally limited hydrometeorological monitoring networks, and few long-term comprehensive hydrologic analyses (Calderón, 2015). Combined, these factors result in poorlydefined local flood information that can lead to greater economic loss and loss of life (Hall et al., 2014).

Data limitations increase erroneous information which can lead to severe financial, environmental, and social consequences. A common approach for estimating peak discharges in ungauged catchments is to apply channel morphometric properties and regional parameters to calibrate hydrologic models. Relying solely on traditional hydrologic monitoring and modeling – which for this paper is described as instrumental records (i.e., weather stations, stream gauges), hydrologic equations, models, and GIS – can lead to several assumptions. For example, single-point instrumental records do not have the temporal frequency to accurately determine extreme flood recurrence and are insufficient to capture spatial flood information within a catchment, such as flow paths, geomorphic changes, and variability of flooding (Starkey et al., 2017). Peak discharges – or maximum extent and depth of floods – are empirically-derived or determined from stream gages to estimate flood frequency. However, these methods oversimplify parameters and produce highly uncertain local estimates (Petroselli, Vojtek, & Vojtekova, 2019). Simulated outputs derived from these data are often the main source of flood knowledge that informs water resource policy and decision making (i.e., 100-year floodplain and flood insurance).

Furthermore, local management decisions are often based on regional flood models that rarely incorporate local flood knowledge (Johnson, 2002). Watershed development projects in data-limited regions often perform poorly due to false assumptions that techniques from one location will be as

applicable in another location with little recognition of local flood knowledge (Johnson et al. 2002). Thus, there is an urgent, ongoing need for better local flood characterization in data-limited regions.

These challenges suggest the need to consider approaches at the right scale and scope to address water resource issues. Previous studies have identified a multitude of alternative methods, with several studies focusing on reducing uncertainty, improving accuracy, and extending beyond instrumental records to include longer-term and extreme flood information (Brázdil et al., 2006; Davis et al., 2019). Metrics, such as root mean square error (RMSE) and comparison of observed and simulated discharges, can be used to assess the reliability of model predictions that can, themselves, be updated (lav et al., 2012). Real-time information from large or flash floods is difficult to capture, thus, quantitative field data and qualitative observations can be used for key inputs of a storm hydrograph (Table 1). These data can calibrate and constrain the simulated flood when traditional hydrologic data are unreliable. This study represents a novel mixed methods approach that combines paleohydrology methods and human observations to construct post-storm hydrographs of an extreme flood. The main objective of this paper is to demonstrate the feasibility of using local knowledge and proxy measures to generate extreme flood hydrographs of the most recent extreme flood in an ungauged catchment.

Table 1: Data and methods to construct a storm hydrograph.

Hydrograph Component	Input Data Description	Traditional Methods	Alternative Methods
Storm duration	Total time of precipitation	Instrumental records, GIS, model	historical & human observations
Precipitation	Precipitation values	Instrumental records, GIS, model	historical & human observations
Precipitation intensity	Precipitation / unit of time	Instrumental records / time of storm	N/A
Pre-storm discharge	Flow discharge	Instrumental records, model	historical & human observations
Bankfull discharge	Channel slope, Manning's R, Cross-sectional area	Hydraulic equation, GIS	Measured stream cross-section, paleohydrology
Rising limb	Discharge between bankfull and Qmax	Instrumental records, model	N/A
Peak discharge (Qmax)	Flood Stage, Peak Discharge	Equation/model	Paleohydrology, historical & human observations
Falling Limb	Discharge between Qmax and bankfull	Instrumental records, model	N/A
Post-storm discharge	Flow discharge after the storm	Instrumental records, model	historical and human observations
Flood duration	Total time of flow above bankfull discharge	Instrumental records, GIS, model	Measured stream cross-section, historical & human observations

Additional Context			
Flood Magnitude	Return Interval	Instrumental records	Historical & human observations
Sub-watershed variability	Precipitation & flow values across watershed	Multiple monitoring sites / GIS, model interpolation	Historical & human observations
Geomorphic impacts	Topography, elevation, channel properties	GIS	Paleohydrology, historical & human observations
Socioeconomic impacts	Social & economic data	N/A	Historical & human observations

1.1 Paleohydrology

The growing field of paleoflood hydrology uses landscape evidence of past major floods, known as paleoproxy evidence, to determine the maximum extent of flooding in a channel. A majority of paleoflood research has been conducted in temperate climates in gauged catchments. Yet, proxy data can be particularly valuable to reconstruct a flood event and to assess the hydrology of ungauged catchments. Thus, there is opportunity to apply paleohydrology methods in data-limited regions to improve the reliability of current flood assessments.

Peak discharge (Qmax) is an important paleoflood indicator used to understand flooding within a catchment. Qmax can be estimated using paleoproxy evidence, such as debris lines, boulder bars, or high-water marks, to calculate the minimal critical discharge to entrain and move the largest clasts during an event (Costa, 1983; Jarrett & Costa, 1988; Wohl, 1992; Knox, 1993; Fanok & Wohl, 1997; Benito et al., 2004; Baker, 2013; Alexander & Cooker, 2016). The Qmax value obtained from paleostage indicators can be used with channel geometry measures for flood management and for critical infrastructure – such as levees, bridges, and roads – to withstand the largest anticipated flow velocity in the channel. However, Qmax represents a single estimate of peak flow and underestimates discharge by up to 20% (Lam et al., 2017). However, paleoflood estimates are insufficient to determine the duration and timing of a flood.

1.2 Qualitative Evidence

Qualitative data, used alone or combined with other methods, can provide spatio-temporal information during and immediately following flood events (Zanon et al., 2010; Hlavcova et al., 2016; Rollason et al., 2018). There is a growing trend of using human observations and historical records to verify, compliment, and improve predictions of flood occurrence and damage from instrumental flood records and conventional hydrologic models (e.g., Assumpção et al., 2018; Borga et al., 2019; Avellaneda, et al., 2020; Etter et al., 2020; Nardi, et al., 2021). Additionally, several studies highlight the benefits of using human observations as a source, rather than as an adjunct to traditional data to improve

data scarcity and accuracy in data-limited regions (e.g., Walker et al., 2016; Njue et al., 2019; Nigussie, et al., 2020, among others). Benefits include engaging, collaborating, and actively involving local communities to improve local monitoring networks, produce new landscape perspectives, and fundamentally contribute to innovative solutions to reduce flood risk. Additionally, observational data can provide consistent information, including estimated flood magnitudes and frequencies, to better predic?t the likelihood of future flood events (Brázdil et al., 2006; Goodchild, 2007; Raska & Brazdil, 2015; Assumpção et al., 2018).

Yet, there is little guidance for interpreting qualitative information to improve estimates of flood magnitude and duration (Poser et al., 2008; Mazzoleni, Amaranto, & Solomatine, 2019). Observations cannot be calibrated, respondents may interpret observations differently, and dates and times are more difficult to recall as time passes after a catastrophic event. Uncertainty can propagate with inaccurate human perception and memory, small sample sizes, and with high variability in responses. Personal biases in data collection and interpretation further amplify uncertainty. However, using traditional methods alone produce high temporal uncertainty of local flood discharge, including peak discharge, when compared to community-based observations or when these methods are combined (Starkey et al., 2017).

Immediately after extreme flood events, post-event surveys from directly impacted individuals could provide detailed estimates on flood duration, flood stage, flow paths, geomorphic impacts, and increase confidence in Qmax estimates (Gaume & Borga, 2008; Marchi et al., 2009; Blaškovičová et al., 2011; Pekárová et al., 2012; Walker et al., 2016; Starkey et al., 2017; Etter et al., 2020). Furthermore, these data can be quantified, averaged, and used – in conjunction with other data sources – to create hydrographs. For example, post-event surveys can estimate the lag time and shape of flood hydrographs that would otherwise be unavailable in short-term records or ungauged catchments (Hlavcova et al., 2016). Additionally, affected locals can create new knowledge about impacts and flow paths (Rollason et al., 2018).

2. Case Study: the Ostional catchment in the Rivas Provence of Nicaragua

The study area lies within the Pacific Coastal Plain of Nicaragua bounded to the west by the Pacific Ocean and by Lake Nicaragua to the east (Figure 1). Twelve ephemeral-to-seasonal, mid-sized Pacific coastal catchments, oriented northeast to southwest, extend south of Managua to Nicaragua's southern border and have associated groundwater aquifers and coastal mangroves. The underlying geology is the

sedimentary Brito Formation, with elevations ranging from sea level to approximately 230 m.a.s.l. (Arengi and Hodgson, 2000; Calderón, 2015). The mean annual precipitation is at least 1,000 mm and mean monthly temperatures above 20°C (WMO, 1983). Seasonally, this region experiences a dry season from November through April followed by a wet season from May through October. A canícula, or dry interval, interrupts the wet season from late July through early August. The dominant land cover types in this region are tropical wet/dry forest and agricultural lands.

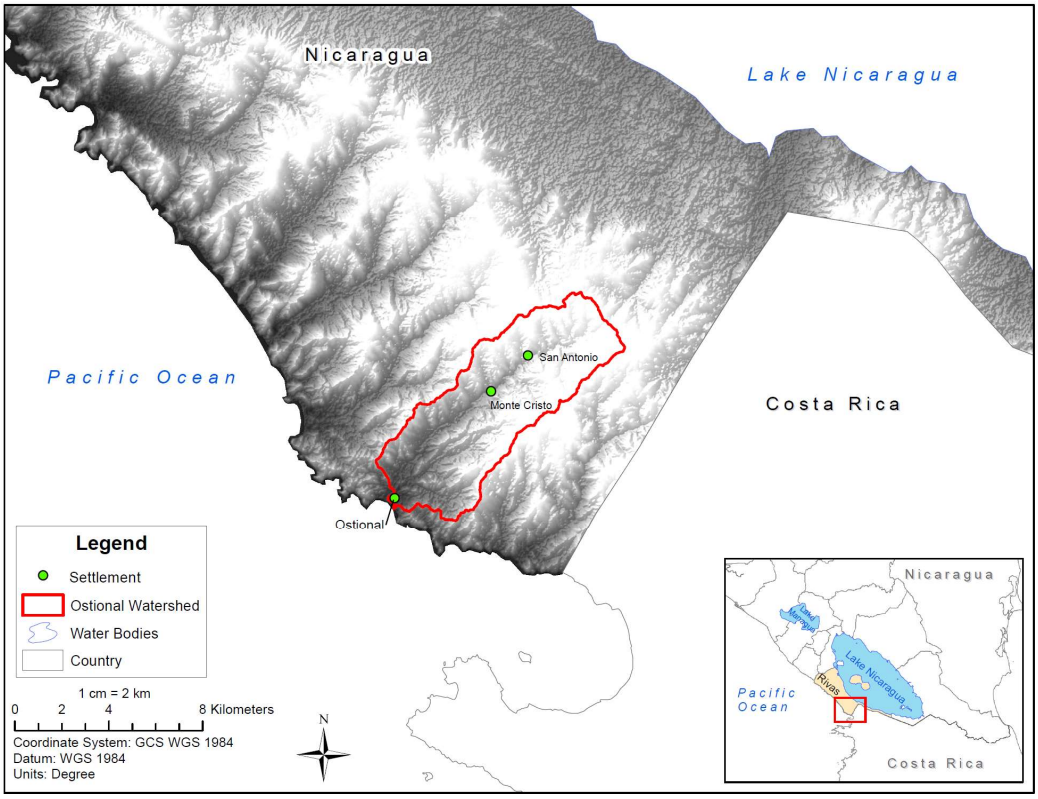

Figure 1: Study Location of the Ostional Catchment in Rivas, Nicaragua.

The Ostional catchment was selected due to its degree of similarity to other Pacific Coastal catchments, the relatively unmodified landscape, limited hydrometeorological information, and a recent extreme flood event. The Ostional catchment is approximately 10 km long with 40 km2 area. At the lowest channel reach less than 1 km away from the coast, the Ostional River flows seasonally, is influenced by groundwater, and has a mangrove estuary (Calderón, 2015). A small fishing community, Ostional, exists near the main channel outlet, with a bridge that crosses the channel to provide town access. Approximately 5.2 km from the coast, the Ostional River runs ephemerally through the rural community of Monte Cristo. Here, the ephemeral channel narrows and deepens near the base of the hilly

landscape above sandstone bedrock and alluvium at elevations greater than 50 m.a.s.l., The rural community of San Antonio is located near the headwaters, approximately 6.8 km from the coastline at an elevation exceeding 70 m.a.s.l.

2.1 Overview of Tropical Storm Nate (October 2017)

In October 2017, a tropical depression developed off the Caribbean coast of Costa Rica and intensified into Tropical Storm Nate as it moved north over the Nicaraguan coastline. Tropical Storm Nate formed on October 3, and had well defined circulation as a tropical depression by October 4. The depression was upgraded to a tropical storm and made landfall in NE Nicaragua at 12:00 PM UTC on October 5 (NHC, 2018). The regional meteorological phenomenon is critical to understanding why the Pacific Coastal Plain is severely impacted by tropical cyclones that form in the Caribbean. Development of Tropical Storm Nate in the Caribbean pulled moisture and winds across the low-lying, narrow plain and Lake Nicaragua, which caused Pacific coastal storm surge, extreme rain, and flooding (Figure 2). Tropical Storm Nate caused extreme precipitation and flooding which devastated local communities and led to 16 deaths in Nicaragua (NASA, 2017).

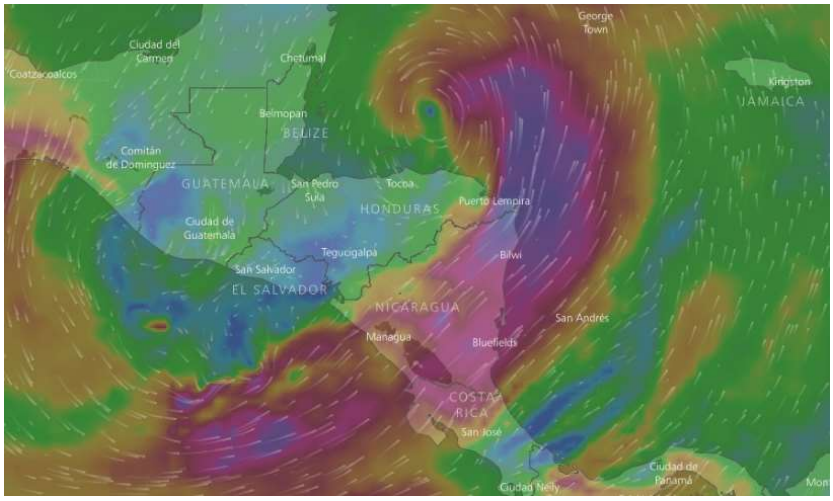

Figure 2: Map of strong pacific winds moving across Nicaragua on October 5, 2017. Reprinted with permission from Windy.com.

3. Methods

3.1 Paleohydrology proxy measures

In the study area, paleohydrology proxy evidence is preserved for several months due to infrequent extreme floods and ephemeral flow. Paleoproxy evidence of the 2017 extreme flood was visible during the 2018 - 2019 field surveys (Figure 3). Channel cross-sections were collected using a terrestrial laser scanner in river reaches near all three communities to determine in-channel hydraulic properties. Multiple proxy measures, such as height of debris lines and boulder bar measurements, were also recorded to estimate flood stage.

Figure 3: a) Paleoproxy evidence of large-magnitude flooding and b) boulder bar measurements within the Ostional River, Nicaragua.

The average maximum flow velocity was reconstructed from a velocity equation of the minimum critical discharge required for floodwaters to entrain and transport the largest boulders within a channel reach. The B-axis measurements of the five largest boulders in each boulder bar were collected and averaged for the competent-depth equation (Costa, 1983):

$$\bar{\upsilon} = 0.18\ d_I^{0.4587} \quad (1)$$

Equation 1 computes the average velocity ($\bar{\upsilon}$) of a flood in steep channels using the average B-axis of the five largest boulders (d_l) moved by the flood. A standard coefficient is based on particle sizes. The 0.4587 exponent is between the 2.6 power law (Nevin, 1946; Fahnestock, 1963) and "sixth power law" (Brahms, 1753; Sternberg, 1875) exponents of average velocity thresholds of particle movement in water. The average depth is estimated from an equation by Costa (1983) that rearranges the Manning formula (Williams, 1983) to solve for average depth (D):

$$D = [\bar{\upsilon}\, n/\sqrt{S}]^{0.5} \quad (2)$$

Flow was assumed to be steady and uniform. S is the average channel slope at the river reach and the Manning's roughness value (n) was estimated based on channel roughness and bedload grain size and shape (Barnes, 1967).

Sixteen cross-sections – nine in San Antonio, four in Monte Cristo, and three in Ostional – were averaged for each reach to estimate the maximum flood velocity, stage, and discharge. Average slope was calculated by subtracting the minimum channel elevation of the lowest cross-section divided by the distance between the first and last cross-section within each reach. The mean reach depth and average channel width were determined by averaging the mean depth and width of cross-sections within a reach.

The minimum critical discharge, determined from the critical-depth equation, was used as an estimation of peak discharge. To determine peak discharge in cubic meters per second (cms), the continuity equation (Equation 3) was used:

$$Q = A*v \quad (3)$$

Q is peak discharge. A is the cross-sectional area of width times the mean depth in m2. The average streamflow velocity (v) is in meters per second (m/s) (Jarrett, 1987). The critical velocity equation (Equation 4) is derived from the Froude Number equation of critical flow in open channels based on the ratio of inertial and gravitational forces (Trivino, 2018). Critical flow was assumed to equal one. If the slope between two cross-sections was less than 0.01, v was multiplied by a constant of 0.85, assumed to be sub-critical flow (Trivino, 2018):

$$v = \sqrt{g * d} \quad (4)$$

Critical velocity is v, g is the acceleration due to gravity (9.81 m/s2), and d is the mean flow depth (m). The flood depth and peak discharge for every cross-section was averaged for each reach, along with

241 the average bankfull discharge. Paleoflood estimates were compared to qualitative survey peak flood
242 depth estimates in Table 4 (Results).

243 **3.2 Household survey data**

244 Between 2018 and 2019, 32 non-random household surveys were conducted within the three towns in
245 the Ostional catchment. This study survey was distributed to households directly impacted by the October
246 2017 flood located within 50 meters of the Ostional River and was exempt from Institutional Review
247 Board approval (IRB Exemption No. 1402793-2). There are more than 30 households in Ostional, while
248 the other two communities each have less than 20 households. Thus, a sample size greater than 30 was
249 appropriate. Surveys were conducted and recorded in Spanish in a private setting with a native Spanish
250 translator present. Informed consent was orally obtained from all study participants, participation was
251 voluntary, and identifying information was anonymized. Survey responses were transcribed with
252 annotations, translated into English, and converted into a quantitative format.

253 Because memories of the extreme Tropical Storm Nate flood were fresh, survey responses provide
254 first-hand observational data. Survey questions included 1) date the rainfall began, 2) the hour rainfall
255 began, 3) the date the rainfall ended, 4) the hour the rainfall ended, 5) the date the flood began, 6) the
256 hour the flood began, 7) the hour the flood peaked, 8) the peak flood stage, 9) flood duration, 10) the
257 flood end date, and 11) whether any previous storms had a similar or greater magnitude than Tropical
258 Storm Nate. The flood duration and flood end date were asked separately to distinguish between when the
259 water receded back into the channel (flood duration) and when the flow conditions returned to normal
260 (flood end). For peak flood stage, respondents provided height estimates based on flood lines in houses
261 from the ground (Figure 4).

262 To analyze and convert survey data into hydrographs, respondents were cataloged by row and
263 responses to each question were converted into qualitative values and placed into columns.
264 Inconsistencies and responses that could not be converted into quantitative values were identified and
265 removed. To estimate peak flood stage for comparison to paleoflood data and to use for hydrographs,
266 survey estimated heights were added to the average depth of channel reaches determined from channel
267 cross-sections. To estimate velocity from survey data, the critical velocity equation was used.

Figure 4: Photo evidence of flood peak stage from a) household surveys, b) indoor water stains, and c) flood water marks on houses.

3.3 Statistical analysis

Central tendencies were measured and assessed for each survey question – start of rainfall, flood start, peak flood stage, end of rainfall, flood duration in hours, and flood end date – to produce descriptive statistics of all surveyed households (Jansen, 2010). An ANOVA univariate variance t-test determined deviations from a normal distribution and confidence interval for each question within the sample (Creswell, 2014). The mean timing of rainfall and flooding, the height of peak flooding, and flood duration were also analyzed based on location (Ostional, Monte Cristo, and San Antonio). The sample mean flood variables for each town were averaged and compared to the sample mean to determine the z-score for a 95% confidence level (*P-value* = 0.05).

3.4 Hydrograph variables

Flood hydrographs were reconstructed for all three Ostional River reaches. Time values were created by combining the mean date and hour values from Table 3 for rain start, flood start, flood peak, flood duration, and flood end. Discharge values were derived from cross-sectional areas and average in-channel flow depths for pre-event baseflow, bankfull discharge, peak flood discharge, and post-event baseflow. The average depth and cross-sectional area of hypothetical low flows were used for pre-event baseflows. Average bankfull discharges, used for the flood start and flood end discharge values, were estimated from

the average depth and cross-sectional area of each reach. Peak flood discharges were determined from Table 4. Post-event discharges were estimated to represent a velocity between bankfull and pre-event discharge.

4. Results

4.1 Household surveys

Survey results are generally consistent with the National Hurricane Center (2018) timing and duration of rainfall and flooding from Tropical Storm Nate. Table 2 shows the descriptive statistics of surveyed households. Of the 32 surveyed households, 68% of respondents were female and 32% were male, likely due to men working outside of the home. The mean respondent age was 42.6 years old, with the oldest being 81 years old and the youngest being 17. The mean household size was 4.7 people, with the highest mean at 5.4 people per household (pph) in San Antonio, followed by Monte Cristo (5.1 pph), and the lowest in Ostional (3.3 pph).

Table 2: Descriptive statistics of surveyed households.

Variable	Ostional (n=9)	Monte Cristo (n=9)	San Antonio (n=14)	Full Sample (n=32)
Mean Age of Head of Household	48.8	44.3	38.8	42.6
Mean Household Size	3.3	5.1	5.4	4.7
Number of Male Respondents	2	2	5	9
Number of Female Respondents	7	7	9	23

Table 3 shows the sample statistics for each question for all 32 household surveys. The mean rain start of October 4 at 9:07 PM is significant and differs by less than an hour from the median and mode. The mean flood start of October 4 at 11:56 PM is within 1 hour of the median and mode. The mean flood peak of October 5 at 11:05 AM is more than 10 hours after the median and mean. The large difference between the mean and other central tendencies for the peak flood value is due to the range of responses between October 4 and October 7 and a positive skewness. Furthermore, two outliers of November 4 and 5 were excluded due to their inconsistency with dates provided for other questions and were likely errors. The mean rain end of October 5 at 11:20 PM differs from the median of October 6 at 2:00 AM, which differs by less than 3 hours. There is no value for the mode, since all values differed from each other. The 2.9 m mean peak flood stage above the floodplain ground is 0.9 m greater than the median and mode. The mean flood duration of 20.6 hours 3.4 hours earlier than the mode, but is larger than the median of 9

hours, indicating a large range and variance in responses. The mean flood end of October 8 at 6:00 PM is similar to the median but is 2.75 days later than the mode.

Table 3: Sample statistics (s=32) of October 2017 flood information.

	Rain Start DD:HH	Flood Start DD:HH	Flood Peak DD:HH	Rain End DD:HH	Flood Duration (Hrs)	Flood recede DD:HH	Flood Height (m) [a]
Mean	10/4 9:07 PM	10/4 11:56 PM	10/5 11:05 AM	10/5 11:20 PM	20.6	10/8/17 6:00 PM	2.9
Median	10/4 9:30 PM	10/5 12:00 AM	10/5 1:00 AM	10/6 2:00 AM	9	10/8/2017 12:00 AM	2
Mode	10/4 10:00 PM	10/5 12:00 AM	10/5 12:00 AM	#N/A	24	10/6/2017 12:00 AM	2
Sample Variance	0.85	0.13	0.68	0.29	343.97	13.78	2.78
Kurtosis	1.38	7.98	0.22	0.22	-0.49	0.78	-0.98
Skewness	0.01	0.02	0.74	-1.18	0.82	0.99	0.40
Range	3.9	2	3.0	1.5	59	15	5.7
Count	14	17	15	9	27	20	19
Standard Deviation	0.92	0.38	0.82	0.54	18.55	3.71	1.67
Confidence Level (95%)	+/-0.53	+/-0.18	+/-0.46	+/-0.41	+/-7.34	+/-1.74	+/-0.80

$\alpha \leq 0.05$ [a]Flood height represents flood level above floodplain ground

The statistical patterns of survey response data are shown in Figure 5. The temporal trend of survey responses in Figure 5a are generally consistent with an expected timeline of a flood event. The flood start had the least variability in responses, indicating this information is likely the most crucial for survey respondents. The flood recede data show the largest skewed distribution of time, with an outlier of October 18. There was a large range for peak flood height, although ~30% of respondents indicated a height of 2 meters. The flood duration is bimodal with 5 responses indicating a duration of 6 hours and 5 responses indicating 24 hours. The flood peak, flood recede, flood height, and flood duration data are positively skewed. The flood duration has a large distribution. An extreme outlier of 624 hours was removed from the dataset. The flood recede date also has a bimodal distribution of October 7 and October 9, with a possible outlier of October 18.

Interestingly, inhabitants consistently indicated that the 2017 flood was the most devastating in recent history. Of the 31 responses, 93.5% (29) indicated the Tropical Storm Nate flood was unprecedented. One respondent indicated that Hurricane Mitch (1998) and Tropical Storm Juana (2004) were similar, but Nate was stronger and worse. This is remarkable since all respondents lived in multi-generational households in the Ostional catchment their whole lives and experienced Hurricane Mitch, deemed the deadliest hurricane to hit Central America in more than 200 years.

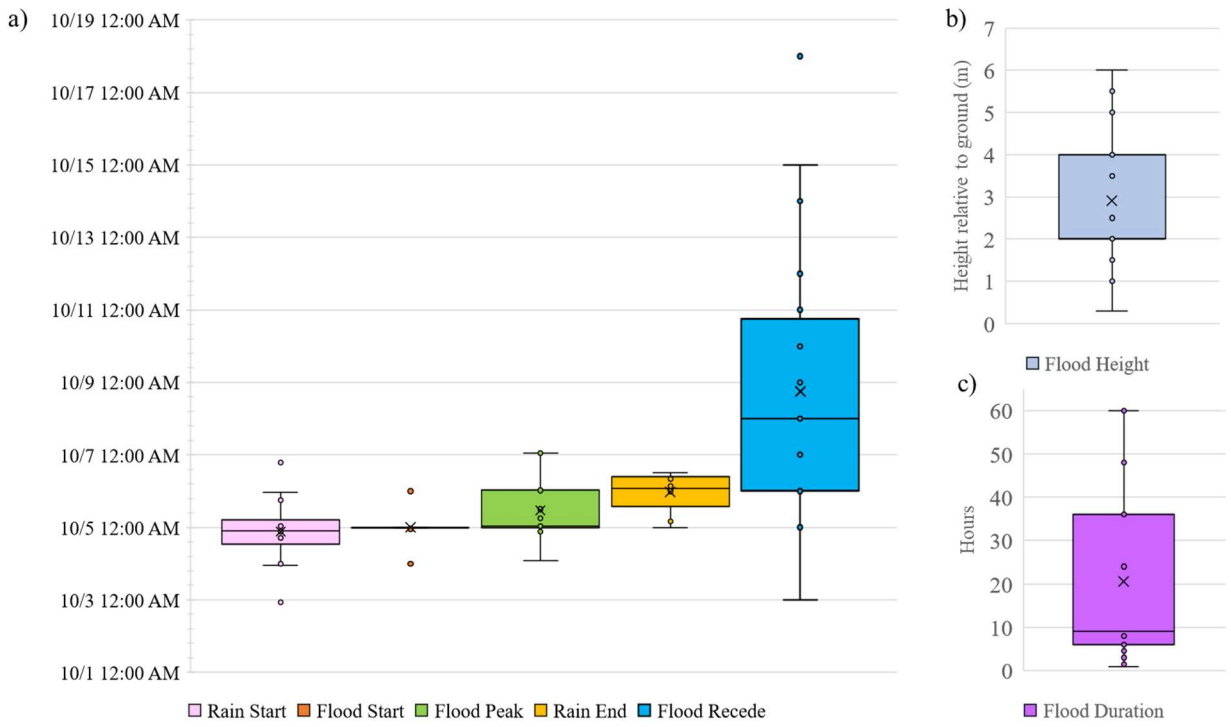

Figure 5: Statistical distribution of sample survey data for the a) event timeline b) peak flood height c) flood duration in hours for the Tropical Storm Nate flood. Each box plot has an X indicating the median, the bottom and upper quartile equally distributed around this value, the mean indicated as a line, the upper and lower extremes indicated by T-bars, and outliers shown as single data points outside of the T-bars.

The mean flood information was also analyzed for each reach (Table 4). All three mean rain start dates matched the sample mean (October 4), with the start hour varying by approximately two hours between reaches. The flood start mean between reaches are all within two hours of the sample mean. Interestingly, the data shows the flood starts earliest in San Antonio, then in Ostional and Monte Cristo, respectively. Although the average means between towns are similar, the value in Monte Cristo was interpolated since only times were provided and there were very few survey responses in Ostional. The comparison of peak flood means between reaches indicates the flood peaked before midnight in San Antonio and after midnight in Ostional and Monte Cristo. The rain ended later upstream in San Antonio compared to in Monte Cristo and Ostional. The only mean variable that was not

The upstream San Antonio reach had an estimated high flood stage of 2.6 m above the bank, while the flood stage was 1.6 m in the lower and flatter Ostional reach, which likely indicates spatial variability. Monte Cristo had highest mean flood stage (3.8 m) and had a longer mean flood recede date (10/11) compared to the other towns. In Ostional, the mean flood duration was quicker than in San Antonio and

Monte Cristo by 11.2 hours and 12.2 hours, respectively. When analyzing the variability across the watershed, it is likely that the flood was flashier and more severe upstream compared to downstream.

Table 4: October 2017 mean flood variables for each town.

	Rain Start DD:HH	Flood Start DD:HH	Flood Peak DD:HH	Rain End DD:HH	Flood Length (Hrs)	Flood Recede Date	Flood Height (m)
Ostional	10/4 8:20 PM	10/4 10:15 PM	10/5 1:45 AM	10/5 7:30 AM	12.25	10/7	1.6
Monte Cristo	10/4 10:30 PM	10/4 10:51 PM	10/5 1:00 AM	10/5 1:30 AM	23.50	10/11	3.8
San Antonio	10/4 9:31 PM	10/4 10:10 PM	10/4 11:48 PM	10/6 3:22 AM	24.45	10/8	2.6
Full Sample	10/4 9:07 PM	10/4 11:56 PM	10/4 11:05 AM	10/6 2:15 AM	20.56	10/8	2.9

4.2 Paleohydrology

The alignment of paleoproxy and household survey results indicate the October 2017 extreme flood is likely the largest magnitude flood that has occurred in at least 75 years in the catchment. The paleoflood estimates for each reach in the Ostional River are shown in Table 5. Although the channel elevation drops significantly between the three reaches, the average slopes at each reach were relatively flat and straight. For all cross-sections, the channel width variance was 6.7 m from the mean ($\bar{x}$ = 5.7 m). The mean channel depth is greatest at Monte Cristo (2.5 m), but all mean reach depths are within a 0.5 m range (0.1 m variance). The average cross-sectional areas are also similar, but have a greater variance of 37.1 m. The paleo velocity calculations are lowest in the San Antonio reach (4.2 m/s) and highest mid-catchment in Monte Cristo (4.8 m/s), both of which correlate with channel slope and channel roughness. The estimated paleoflood stage is extreme, with all three reaches exceeding five meters. The estimated maximum flood discharge was highest in Monte Cristo (599 cms), followed by 520 cms in Ostional, and 511 cms in San Antonio. The variance was 4688 cms and the standard deviation was 68.5 cms.

Table 5: Paleohydrology Flood Estimates of the October 2017 Storm Event in Ostional.

River Reach	Distance from Coast (km)	Minimum Channel Elevation (m)	Average Slope (m/m)	Manning's n	Average Channel Width (m)	Mean Depth (m)	Average Cross-Sectional Area (m^2)	Paleo Velocity (m/s)	Paleo Flood Stage (m)	Max Q Estimate (cms)
San Antonio	6.9	70.9	0.01	0.58	57.5	2.0	119.5	4.2	5.1	511
Monte Cristo	5.2	51.3	0.01	0.70	52.2	2.5	122.5	4.8	5.6	599
Ostional	0.7	11.2	0.00	0.30	54.7	2.3	120.4	4.3	8.6	520

The estimated peak flood depth and velocity from the competent-depth method, boulder bar estimates, and household survey responses are shown in Table 6. The flood depths from all three methods show an upstream to downstream trend, apart from human observations in Ostional. In Ostional, the flood depths had a sample variance of 5.2, with the largest % difference between the Ostional household survey estimate and the competent-depth estimate (18.1%) and boulder bar estimate (11%), respectively. The larger difference in human observed flood stage estimates to paleoflood estimates is likely due to both fewer and wider range of survey responses. The Ostional boulder bar and competent depth estimates differ by 7.6%. The estimated depths varied the least in the San Antonio reach (0.2 variance), with the human observed estimate differing by 0.8% from the competent-depth estimate and 3.9% from the boulder bar estimate. The boulder bar and competent-depth estimates in San Antonio differed by 2.7%. In Monte Cristo, the estimated flood stage also had a variance of 0.2, with a 1.3% difference between the competent-depth and human observation estimates, a 2.7% difference between the boulder bar and competent-depth estimates, and a 4% difference between the boulder bar estimates and human observations.

Table 6: Comparison of Peak Flood Estimates of the October 2017 Storm Event.

	Competent-Depth		Boulder Bar		Human Observations	
River Reach	Velocity (m/s)	Depth (m)	Velocity (m/s)	Depth (m)	Velocity (m/s)	Depth (m)
San Antonio	4.2	5.1	3.1	4.5	6.6	5.2
Monte Cristo	4.8	5.6	3.9	5.0	7.0	5.9
Ostional	4.3	8.6	1.7	6.3	5.8	4.0

The human observed peak flood velocities were consistently the highest, while the boulder bar estimates were consistently the lowest, primarily due to different equations. Human observations provided a depth estimate; thus, the velocity was determined using the critical velocity equation. Furthermore, both the boulder bar and competent-depth estimates represent lower-limit velocity thresholds. In the Ostional reach, the boulder bar estimated velocity is significantly less than the estimated velocities from the competent-depth method (21.8% difference) and human observations (27.3% difference). The boulder bar velocity is directly proportional to the average b-axes of the largest boulders and is greatly influenced by slope. The b-axes were significantly smaller in the Ostional reach than upstream; however, the Ostional reach has a very flat slope (0.1%) that requires a greater flow depth to have adequate force to entrain the boulders.

4.3 Storm hydrographs

Flood hydrographs were reconstructed for each reach within the Ostional catchment (Figure 6). In San Antonio, the storm began on October 4 at 9:31 PM with a pre-event baseflow of 55 cms. The flood began at 10:10 PM with a discharge estimated at 256 cms. An hour and a half later, the flood peaked at 511 cms. The flood, lasting 24.5 hours, receded into the channel at approximately 12:18 AM on October 7. The estimated post-event flow was 140 cms on October 8. Monte Cristo, the 'flashiest' hydrograph, had the highest estimated flood stage and discharge, and the slowest retreat of flow. The rain began on October 4 at 10:30 PM with a pre-event baseflow of 28 cms. Discharge exceeded bankfull (161 cms) by 10:51 PM on October 5 and quickly peaked at 1:00 AM (599 cms) the next morning. The discharge receded below bankfull 23.5 hours later, and the post-event flow (95 cms) occurred on October 11. The Ostional hydrograph is similar to the San Antonio hydrograph with the rain beginning on October 4 at 8:20 PM and a pre-event baseflow of 38 cms. At 10:15 PM, the flow exceeded bankfull discharge (333 cms) and peaked at 1:45 AM on October 5 with a discharge of 520 cms. The discharge was quickest to recede (12.3 hours later) and became post-storm flow (163 cms) on October 7. Peak flooding in Ostional occurred when tides were low, indicating that the tides did not substantially affect coastal flooding, but provides reasonable explanation for why the flood receded faster in Ostional than further upstream (Supplemental Data).

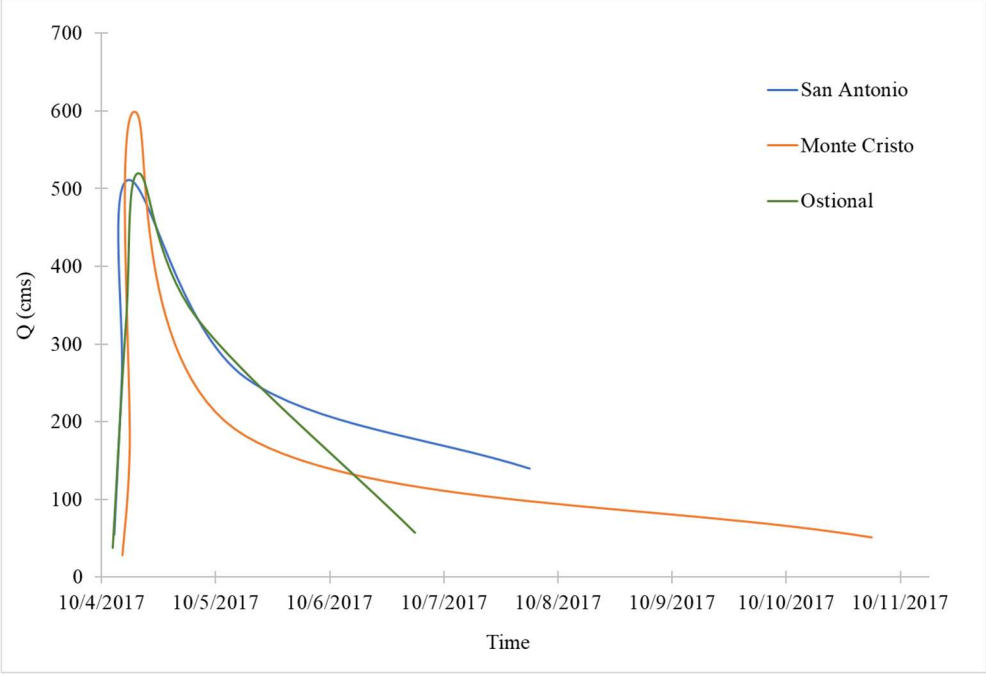

Figure 6: Reconstructed October 2017 flood hydrographs for all three reaches.

5. Discussion

5.1 Mixed methods

This study demonstrates the feasibility of using mixed paleohydrology and qualitative survey methods to produce reliable storm hydrographs of an extreme flood event in data-limited areas. Prior to the study, there was not much traditional data and flood characterization in the Ostional catchment. Combined, the paleoproxy measures, household survey data, and storm hydrographs provide robust flood information in a representative ungauged catchment.

The limited measures of flow and event records led to several assumptions. First, we assumed the October 2017 flood was the most extreme in the study catchment. Since paleoflood estimates help determine the maximum flood and not identify a specific event, there could have been a more extreme previous flood. However, evidence – such as height of flood debris, lack of in-channel vegetation, and survey responses – all indicated the Tropical Storm Nate flood was the most recent extreme flood.

Estimates of flood stage and peak discharge varied between the boulder bar, survey, and competent-depth methods. Results show boulder bar estimates of flood stage and discharge were typically lower than the competent-depth and survey estimates. However, boulder bar estimates describe the lower limit of flooding with up to 20% inaccuracy; thus, these estimates likely correspond to the minimum flood stage and discharge that occurred during the flood. Paleoflood calculations from average slope, roughness, and cross-sectional geometry contribute to uncertainty and remain an important challenge for applying this method (Brázdil et al., 2006; Davis et al., 2019). When paleoflood calculations were combined with descriptive data, water stage estimates ranged from 0.8% to 4% difference in the San Antonio and Monte Cristo reaches. Thus, indicating that mixed methods are considerably useful to verify and improve the accuracy of paleoflood peak flow estimates (Brázdil et al., 2006).

Survey results demonstrate the reliability of qualitative methods to provide crucial spatial and temporal aspects of the flood. Memories of the 2017 extreme flood were recent enough to provide consistent post-flood timing and duration data (Rollason et al., 2018). Interestingly, the most consistent survey responses were the time of peak flooding and that the 2017 flood was more severe than past floods, which is useful for extreme flood recurrence in the Ostional catchment. It is likely that the most recent and traumatic flood could have skewed perception of past floods. However, 93% of survey

responses is a strong indicator of validity that the 2017 flood was the most devastating in the past 40 to 80 years, based on median and oldest age of surveyed population, and likely even longer.

Results demonstrate central tendencies of flood variables are useful to assess inconsistency in survey responses and to establish a general timeline of local flooding. However, converting qualitative data into quantitative values is challenging. Not every survey question was answered, nor respondents may not have understood or responded in the intended way, which affects the sample statistical patterns and error estimations. Unanswered questions or responses that could not be converted into a numerical format, such as days of the week or "it rained all month," were excluded. The flood end date had the most widely variable responses, likely due to multiple factors, such as survey question design, respondents' interpretation of the question, and the ambiguity of defining the end of a flood. Consideration should also be given when interpreting the data. Since the dates and hours were combined in this study, this likely affected statistical measures. Measures of central tendency provide precise flood information for most survey responses but were not as effective for questions with very few responses or with non-Gaussian data. Other methods, such as cluster analyses and cross-tabulation, may provide additional information.

Although it is not possible to distinguish between spatial and human uncertainty, results highlight the variability in the timing and duration of rainfall and flooding within the upper, middle, and lower river reaches that was not previously identified. The variation of mean flood duration and flood end dates between the three reaches could indicate differences in topography and microclimates between the coast and upstream. The flood may have receded quickest in Ostional due to the retreat of coastal storm surge to allow floodwaters to drain seaward. The longer flood in Monte Cristo is likely due to the narrowing and deepening of the channel to funnel and concentrate floodwaters where the slope begins to flatten. This information is highly valuable to improve understanding of extreme and flash flood events not typically captured using traditional monitoring methods.

The knowledge and experiences of local communities of past floods is an invaluable data source that provides a more holistic understanding of flood pathways and timeline in an ungauged basin compared to traditional data (Blue & Brierley, 2015; Lane, 2017; Rollason et al., 2018). Respondents provided additional information on channel erosion and movement, property damage and loss, secondary health effects, flood response and aid, and personal narratives. Although these data were not analyzed in the study, they are invaluable to understand how local communities were affected, the local flood perception and risk, and the flood response and management structure. As 'knowledge holders,' locals provide

understanding of landscape and flooding beyond traditional data sources and help provide narrative and alternative viewpoints seldomly incorporated in flood management (Stocking, 1995; Starkey et al., 2017).

5.2 Hydrographs

Storm hydrographs are commonly derived from a single-point continuous measure of flood stage or discharge to determine the timing, duration, and severity of flooding within a catchment. However, instrumental records often do not distinguish flood information in different reaches nor can be used to develop storm hydrographs in ungauged catchments. Based on an extensive literature review, this study is likely the first to combine household surveys and paleoproxy data to reconstruct extreme flood hydrographs in an ungauged catchment. Human observations provide daily and hourly flood estimates for five requisite points of lag time, rising limbs, and falling limbs critical to construct hydrographs. These data also provide a better understand the rainfall-runoff relationship to construct the hydrographs.

The anecdotal and paleohydrology methods and results of this study provide evidence of how floodwaters moved downstream and how changes across the Ostional channel affected this movement. Results indicate that the Monte Cristo reach had the flashiest hydrograph, which aligns with measured morphometric properties of the reach. Furthermore, the flood in the Ostional reach receded approximately 12 hours faster. These findings diverge from the general understanding of flow behavior of higher discharge as the channel widens in the lower reaches of a catchment. However, flood discharge can vary drastically in different parts of the channel due to multiple factors, such as land cover, geomorphic properties, and infiltration rates. We theorize that a break in channel gradient caused floodwaters to concentrate in Monte Cristo and likely caused channel incision, erosion, and migration.

Determining the accuracy of the hydrographs is challenging since there was no information on baseflow conditions, field measurements were averaged, and peak values were estimated. Despite the likelihood of hydrograph components being overestimated or underestimated, they are valuable for critical infrastructure to withstand extreme floods, to improve flood management, and to prepare for more variable and extreme events (Bouleau, 2014; Ashmore, 2015; Lane, 2017). When data from multiple sources indicate similar outputs, ambiguity is reduced, and confidence increases. Collectively, the paleoproxy and household survey data provide a robust estimate of the timing and duration of precipitation and discharge from Tropical Storm Nate, decrease uncertainty from paleostage indicators, and more accurately calculate the rising limb, falling limb, and peak stage of the storm hydrographs.

6. Conclusion

This study is one of the first aimed at integrating mixed paleoproxy measures and household survey data to provide reliable estimates of the largest floods expected in an ungauged catchment in a data-limited region. The methods provide reasonable estimates of the duration, magnitude, and upper limits of extreme flooding that are also useful in gauged catchments, as many systematic instrumental records fail to provide relevant information on the magnitude of catastrophic events (Brázdil et al., 2006). Household surveys can suitably estimate the timing and duration of a recent extreme flood event and can be verified from historical records. When combined with paleoflood data, uncertainty in peak discharge can be reduced. Moreover, these data can identify spatio-temporal variability of rain and flooding between the upper, middle, and lower river reaches. Combined, these data can provide daily-to-hourly extreme flood information that can be used to reconstruct extreme storm hydrographs. Five data points provide sufficient information on the hydrograph's shape, lag-time, peak discharge volume, and receding time to better understand flow response from large storm events.

This study provides a baseline assessment of an extreme flood to improve local flood management and infrastructure development and can be adapted for any catchment. Furthermore, this study provides circumstantial evidence of flood recurrence and how more intense flooding could occur in the future, since respondents indicated that this extreme flood, produced from a tropical storm, was similar, but more intense, than flooding from past hurricanes. To conclude, the benefits gained from engaging with and involving local communities, such as enhancing community resilience and management, improving data availability, and reducing data uncertainty are invaluable (Johnson et al., 2002; Starkey et al., 2017). Thus, incorporating local observational data enhances understanding of the local flood context and community structure to improve research and water resource management that benefit those most vulnerable to flooding.

Acknowledgements: The authors express gratitude for the collaboration between the University of Denver and the National Autonomous University of Nicaragua (UNAN-Managua) for the resources for the first author to conduct her research. This research was supported by funding by the National Science Foundation Human-Environment Geographical Sciences Doctoral Dissertation Research Improvement Award #21276027, University of Denver Geography Department and LatinX Center, the American Association of Geographers (AAG), the AAG Geomorphology Specialty Group, the GIS Colorado Professional Group, and by UT-Battelle, LLC, under contract DE-AC05-00OR22725 with the US Department of Energy (DOE) and US DOE Office of Science Early Career Research program as part of research in Earth System Model Development within the Earth and Environmental Systems Modeling Program.

CRediT author statement: Shannon Jones: Conceptualization, Methodology, Funding Acquisition, Investigation, Formal Analysis, Writing – Original Draft; Heyddy Calderón: Conceptualization, Methodology, Supervision, Resources, Writing – Review & Editing.

Data Availability Statement: All quantitative data that support the findings of this study are available within the paper and its Supplementary Information files. The translated, transcribed, and anonymized household survey data are publicly available as open data via the Qualitative Data Repository (QDR) online data repository at Syracuse University. https://doi.org/10.5064/F6ELHKCS. The US government retains and the publisher, by accepting the article for publication, acknowledges that the US government retains a nonexclusive, paid-up, irrevocable, worldwide license to publish or reproduce the published form of this manuscript, or allow others to do so, for US government purposes. DOE will provide public access to these results of federally sponsored research in accordance with the DOE Public Access Plan (https://www.energy.gov/doe-public-access-plan).

7. References

Alexander, J., & Cooker, M. J. (2016). Moving boulders in flash floods and estimating flow conditions using boulders in ancient deposits. Sedimentology, 63(6), 1582–1595. https://doi.org/10.1111/sed.12274

Arengi, J., Hodgson, G. (2000). Overview of the geology and mineral industry of Nicaragua. International Geology Review. 42(1), pp. 45–63.

Ashmore, P. (2015). Towards a sociogeomorphology of rivers. Geomorpology. https://doi.org/10.1016/j.geomorph.2015.02.020

Assumpção, T. H., Popescu, I., Jonoski, A., & Solomatine, D. P. (2018). Citizen observations contributing to flood modelling: opportunities and challenges. Hydrol. Earth Syst. Sci, 22, 1473–1489. https://doi.org/10.5194/hess-22-1473-2018

Avellaneda, P. M., Ficklin, D. L., Lowry, C. S., Knouft, J. H., & Hall, D. M. (2020). Improving Hydrological Models with the Assimilation of Crowdsourced Data. Water Resources Research, 56(5), e2019WR026325. https://doi.org/10.1029/2019WR026325

Baker, V. (2013). Global Late Quaternary Fluvial Paleohydrology: With Special Emphasis on Paleofloods and Megafloods. In Treatise on Geomorphology (Vol 9, pp. 511-527). Elsevier Inc. https://doi.org/10.1016/B978-0-12-374739-6.00252-9

Barnes, H. H., Jr., (1967). Roughness characteristics of natural channels. U.S. Geol. Surv. Water-Supply Paper 1849, 213 p.

Benito, G., Lang, M., Barriendos, M., Llasat, M. C., Francés, F., Ouarda, T., Thorndycraft, V., Enzel, Y., Bardossy, A., Coeur, D., & Bobée, B. (2004). Use of Systematic, Palaeoflood and Historical Data for the Improvement of Flood Risk Estimation. Review of Scientific Methods. Natural Hazards, 31(3), 623–643. https://doi.org/10.1023/B:NHAZ.0000024895.48463.eb

Blue, B., & Brierley, G. (2016). 'But what do you measure?' Prospects for a constructive critical physical geography. Area, 48(2), 190–197. https://doi.org/10.1111/area.12249

Blaškovičová, L., Horvát, O., Hlavčová, K., Kohnová, S., Szolgay, J., (2011). Methodology for post-event analysis of flash floods - Svacenický Creek Case Study. Contributions to Geophysics and Geodesy, 41, 3, 235–250. https://doi.org/10.2478/v10126-011-0009-9

Borga, M, Comiti, F, Ruin, I, Marra, F. (2019). Forensic analysis of flash flood response. WIREs Water, 6, e1338. https://doi.org/10.1002/wat2.1338

Bouleau, G. (2014). The co-production of science and waterscapes: The case of the Seine and the Rhône Rivers, France. Geoforum, 57, 248–257. https://doi.org/10.1016/j.geoforum.2013.01.009

Buoyweather (n.d.). October 1-10, 2017. Wave Height and Tides. Retrieved February 19, 2020. www.buoyweather.com

Brahms, A. (1753). Anfangsgründe der deich-und. Wasserbaukunst, Aurich. Retrieved from Costa, J.E. (1986).

Brázdil, R., Kundzewicz, Z. W., Benito, G. (2006). Historical hydrology for studying flood risk in Europe. Hydrological Sciences Journal. 51(5), 739-764. https://doi.org/10.1623/hysj.51.5.739

Calderón, H. (2015). Surface and Subsurface Runoff Generation Processes in a Poorly Gauged Tropical Coastal Catchment: A study from Nicaragua. CRC Press/Balkema. Leiden, The Netherlands.

Costa, J. E. (1983). Paleohydraulic reconstruction of flash-flood peaks from boulder deposits in the Colorado Front Range: Geological Society of America Bulletin. 94(8), pp. 986 -1004. https://doi.org/10.1130/0016-7606(1983)94<986:PROFPF>2.0.CO;2

Creswell, J. W. (2014). Research design: Qualitative, quantitative, and mixed methods approaches (4th ed). SAGE Publications.

Davis, L., Harden, T. M., Muñoz, S. E., Godaire, J., O'Connor, J. E. (2019). Preface to historic and paleoflood analyses: New perspectives on climate, extreme flood risk, and the geomorphic effects of large floods. Geomorphology. 327, 610-612. https://doi.org/10.1016/j.geomorph.2018.10.021

Etter, S., Strobl, B., Seibert, J., & van Meerveld, H. J. I. (2020). Value of Crowd-Based Water Level Class Observations for Hydrological Model Calibration. Water Resources Research, 56(2). https://doi.org/10.1029/2019WR026108

Fanok, S. F., & Wohl, E. E. (1997). Assessing the Accuracy of Paleohydrologic Indicators, Harpers Ferry, West Virginia. JAWRA Journal of the American Water Resources Association, 33(5), 1091–1102. https://doi.org/https://doi.org/10.1111/j.1752-1688.1997.tb04127.x

Fahnestock, R. K. (1963). Morphology and hydrology of a glacial stream White River, Mount Rainier. Washington: U.S. Geological Survey Professional Paper 422-A, 70 p.

Gaume, E., Borga, M. (2008). Post-flood field investigations in upland catchments after major flash floods: proposal of a methodology and illustrations. Journal of Flood Risk Management, 1, 4, 175–189. https://doi.org/10.1111/j.1753-318X.2008.00023.x

Goodchild, M. F. (2007). Citizens as sensors: the world of volunteered geography. GeoJournal, 69(4), 211–221. https://doi.org/10.1007/s10708-007-9111-y

Goodchild, M. F., Glennon, J. A. (2010). Crowdsourcing geographic information for disaster response: a research frontier. International Journal of Digital Earth. 3(3), 231-241. https://doi.org/10.1080/17538941003759255

Gorgoglione, A., Castro, A., Chreties, C., & Etcheverry, L. (2020). Overcoming Data Scarcity in Earth Science. Data, 5(1), 5. https://doi.org/10.3390/data5010005

Gourley, J. J., Erlings, J. M. Smith, T. M, Ortega, K. L, and Hong, Y. (2010). Remote collection and analysis of witness reports on flash floods. Journal of Hydrology. 394, 53-62. https://doi.org/10.1016/j.jhydrol.2010.05.042

611 Gupta, H. V., Clark, M. P., Vrugt, J. A., Abramowitz, G., and Ye, M. (2012). Towards a comprehensive
612 assessment of model structural adequacy, Water Resource Research. 48, W08301.
613 https://doi.org/10.1029/2011WR011044

614 Hall, J., Arheimer, B., Borga, M., Brázdil, R., Claps, P., Kiss, A., Kjeldsen, T. R., Kriauciuniene, J.,
615 Kundzewicz, Z. W., Lang, M., Llasat, M. C., Macdonald, N., McIntyre, N., Mediero, L., Merz,
616 B., Merz, R., Molnar, P., Montanari, A., Neuhold, C., Parajka, J., Perdigão, R. A. P., Plavcová1,
617 L., Rogger, M., Salinas, J. L., Sauquet, E., Schär, C., Szolgay, J., Viglione, A., & Blöschl, G.
618 (2014). Understanding flood regime changes in Europe: a state-of-the-art assessment. Hydrology
619 and Earth System Sciences, 18, 2735-2772. https://doi.org/10.5194/hess-18-2735-2014

620 Hlavčová, K., Kohnová, S., Borga, M., Horvát, O., Šťastný, P., Pekárová, P., Majerčáková, O., &
621 Danáčová, Z. (2016). Post-event analysis and flash flood hydrology in Slovakia. Journal of
622 Hydrology and Hydromechanics, 64(4), 304–315. https://doi.org/10.1515/johh-2016-0041

623 IPCC. (2019). Chapter 4: Sea level rise and implications for low lying islands, coasts and communities.
624 Abe-Ouchi, A., Gupta, K., Pereira, J. (eds). Special Report on the Ocean and Cryosphere in a
625 Changing Climate.

626 Jansen, H. (2010). The logic of qualitative survey research and its position in the field of social research
627 methods. Forum: Qualitative Social Research 11(2), Art. 11. http://dx.doi.org/10.17169/fqs-
628 11.2.1450

629 Jarrett, R. D. (1987). Errors in slope-area computations of peak discharges in mountain streams. Journal
630 of Hydrology. 96(1-4), 53-67. https://doi.org/10.1016/0022-1694(87)90143-0

631 Jarrett, R. D. and Costa J. E. (1988). Evaluation of the flood hydrology in the Colorado Front Range using
632 precipitation, streamflow, and paleoflood data for the Big Thompson River basin: USGS Water
633 Resource Investigations Report 87-4117: 37 p. https://doi.org/10.3133/wri874117

634 Johnson, N., Ravnborg, H. M., Westermann, O., Probst, K. (2002). User participation in watershed
635 management and research. Water Policy, 3(6), 507-520. https://doi.org/10.1016/S1366-
636 7017(02)00014-4

637 Jones, S. 2023. "Mixed-methods approach to flood hydrology in ungauged catchments". Qualitative Data
638 Repository. https://doi.org/10.5064/F6ELHKCS. QDR Main Collection. Draft version.

639 Knox, J. C. (1993). Large increases in flood magnitude in response to modest changes in climate. Nature,
640 361: pp. 430–432. https://doi.org/10.1038/361430a0

641 Kundzewicz, Z. W. (2007). Prediction in ungauged basins—A systemic perspective. 7.

642 Lam, D., Thompson, C., Croke, J., Sharma, A., Macklin, M. G. (2017). Reducing uncertainty with flood
643 frequency analysis: the contribution of palaeo- and historical flood information. Water Resource
644 Research. 53(3), 2312-2327. https://doi.org/10.1002/2016WR019959

645 Lane, S. N. (2017). Slow science, the geographical expedition, and Critical Physical Geography. The
646 Canadian Geographer / Le Géographe Canadien, 61(1), 84–101.
647 https://doi.org/10.1111/cag.12329

Marchi, L., Borga, M., Preciso, E., Sangati, M., Gaume, E., Bain, V., Delrie, G., Bonnifait, L., Pogačnik, N., (2009). Comprehensive post-event survey of a flash flood in Western Slovenia: observation strategy and lessons learned. Hydrological Process., 23(26), 3761–3770. https://doi.org/10.1002/hyp.7542

Mazzoleni, M., Amaranto, A., & Solomatine, D. P. (2019). Integrating Qualitative Flow Observations in a Lumped Hydrologic Routing Model. https://doi.org/10.1029/2018WR023768

Nardi, F., Cudennec, C., Abrate, T., Allouch, C., Annis, A., Assumpção, T., Aubert, A. H., Bérod, D., Braccini, A. M., Buytaert, W., Dasgupta, A., Hannah, D. M., Mazzoleni, M., Polo, M. J., Sæbø, Ø., Seibert, J., Tauro, F., Teichert, F., Teutonico, R., … Grimaldi, S. (2021). Citizens AND HYdrology (CANDHY), conceptualizing a transdisciplinary framework for citizen science addressing hydrological challenges. Hydrological Sciences Journal, 67(16), 2534-2551. https://doi.org/10.1080/02626667.2020.1849707

National Aeronautics and Space Administration (NASA). (2017). GPM examines forming Tropical Storm Nate (TD16). Accessed July 2, 2018. https://pmm.nasa.gov/extreme-weather/gpm-examines-forming-tropical-storm-nate-td16

Nigussie, L., Haile, A. T., Gowing, J., Walker, D., & Parkin, G. (2020). Citizen science in community-based watershed management: An institutional analysis in Ethiopia. IWMI Working Papers, 2020(191), IWMI-1-IWMI-18. https://doi.org/10.5337/2020.207

Njue, N., Stenfert Kroese, J., Gräf, J., Jacobs, S. R., Weeser, B., Breuer, L., & Rufino, M. C. (2019). Citizen science in hydrological monitoring and ecosystem services management: State of the art and future prospects. Science of the Total Environment, 693, 133531. https://doi.org/10.1016/j.scitotenv.2019.07.337

Nevin C. (1946). Competency of moving water to transport debris: Geological Society of America Bulletin. 57, 651-674.

National Hurricane Center (NHC). (2018). Tropical Cyclone Report: Hurricane Nate. Retrieved from https://www.nhc.noaa.gov/data/tcr/AL162017_Nate.pdf

National Centers for Environmental Information (NCEI). (2021). U.S. Billion-Dollar Weather and Climate Disasters. Retrieved from https://www.ncdc.noaa.gov/billions/.

Pekárová, P., Svoboda, A., Miklánek, P., Škoda, P., Halmová, D., Pekár, J. (2012). Estimating flash flood peak discharge in Gidra and Parná basin: Case study for the 7-8 June 2011 flood. Journal of Hydrology and Hydromechanics, 60(3), 206–216. https://doi.org/10.2478/v10098-012-0018-z

Petroselli, A., Vojtek, M., & Vojteková, J. (2019). Flood mapping in small ungauged basins: A comparison of different approaches for two case studies in Slovakia. Hydrology Research, 50(1), 379–392. https://doi.org/10.2166/nh.2018.040

Raska, P. and R. Brázdil. (2015). Participatory responses to historical flash floods and their relevance for current risk reduction: a view from a post-communist country. Area, 47(2), 166-178. https://doi.org/10.1111/area.12159

685 Rollason, E., Bracken, L. J., Hardy, R. J., Large, A. R. G. (2018). The importance of volunteered
686 geographic information for the validation of flood inundation models. Journal of Hydrology. 562,
687 267-280. https://doi.org/10.1016/j.jhydrol.2018.05.002

688 Starkey, E., Parkin, G., Birkinshaw, S., Large, A., Quinn, P., Gibson, C. (2017). Demonstrating the value
689 of community-based ('citizen science') observations for catchment modelling and
690 characterization. Journal of Hydrology. 548, 801-817.
691 https://doi.org/10.1016/j.jhydrol.2017.03.019

692 Sternberg, H. (1875). Zeitschrift für Bauwesen, 25. P. 483. Retrieved from Costa, J.E. (1986)

693 Trivino, N. (2018). Paleoflood hydrology and basin morphometric characteristics related to flooding in
694 the Colorado Front Range (Thesis No. 1427) University of Denver, Department of Geography
695 and the Environment. DU Digital Commons. Retrieved from
696 https://digitalcommons.du.edu/etd/1427

697 Walker, D., Forsythe, N., Parkin, G., & Gowing, J. (2016). Filling the observational void: Scientific value
698 and quantitative validation of hydrometeorological data from a community-based monitoring
699 programme. Journal of Hydrology, 538, 713–725. https://doi.org/10.1016/j.jhydrol.2016.04.062

700 Williams, G. P. (1983). Paleohydrological methods and some examples from Swedish fluvial
701 environments: I cobble and boulder deposits. Geografiska Annaler: Series A, Physical
702 Geography, 65(3-4), 227-243.

703 Wohl, E.E. (1992). Bedrock benches and boulder bars: Floods in the Burdekin Gorge of Australia.
704 Geological Society of America Bulletin, 104(6), 770–778. https://doi.org/10.1130/0016-
705 7606(1992)104%3C0770:BBABBF%3E2.3.CO;2

706 Wohl, E., Barros, A., Brunsell, N., Chappell, N. A., Coe, M., Giambelluca, T., Goldsmith, S., Harmon,
707 R., Hendrickx, J. M. H., Juvik, J., McDonnell, J., & Ogden, F. (2012). The hydrology of the
708 humid tropics. Nature Climate Change, 2(9), 655–662. https://doi.org/10.1038/nclimate1556

709 World Meteorological Organization (WMO). (1983). Operational hydrology in the humid tropical
710 regions. Hydrology of Humid Tropical Regions. Proceedings of SAKS Symposium held during
711 18th General Assembly of IUGG. Hamburg. IAHS Publication 140.

712 Zanon, F., Borga, M., Zoccatelli, D., Marchi, L., Gaume, E., Bonnifait, L., Delrieu, G. (2010).
713 Hydrological analysis of a flash flood across a climatic and geologic gradient. September 18,
714 2007 event in Western Slovenia. Journal of Hydrology, 394(1-2), 182–197.
715 https://doi.org/10.1016/j.jhydrol.2010.08.020

716 Zheng, F., Tao, R., Maier, H. R., See, L., Savic, D., Zhang, T., Chen, Q., Assumpção, T. H., Yang, P.,
717 Heidari, B., Rieckermann, J., Minsker, B., Bi, W., Cai, X., Solomatine, D., & Popescu, I. (2018).
718 Crowdsourcing Methods for Data Collection in Geophysics: State of the Art, Issues, and Future
719 Directions. Reviews of Geophysics, 56(4), 698–740. https://doi.org/10.1029/2018RG00061